



Supplement of

Sea surface temperature evolution of the North Atlantic Ocean across the Eocene–Oligocene transition

Kasia K. Śliwińska et al.

Correspondence to: Kasia K. Śliwińska (kksl@geus.dk) and Agatha M. de Boer (agatha.deboer@geo.su.se)

The copyright of individual parts of the supplement might differ from the article licence.

1. Terminology of the Eocene-Oligocene Transition.

In our paper we have applied terminology suggested in the recent review by Hutchinson et al. (2021). According to the revised definition, the EOT is understood as a phase of accelerated climatic and biotic change that began before and ended after the Eocene-Oligocene boundary (EOB). Stratigraphically the EOT is defined at its base by the extinction of the nannofossil *D. saipanensis* and at its top by the highest values of the benthic $\delta^{18}\text{O}$ maximum referred to as EOIS, which postdates the base of magnetostratigraphic Chron C13n. On the most commonly used current timescale, ‘Geological Timescale 2012’ (GTS2012; Gradstein et al., 2012), the critical levels are calibrated as follows: extinction of *D. saipanensis* = 34.44 Ma; the EOB = 33.88 Ma (the extinction of *Hantinina* spp.); the base of Chron C13n at 33.705, and the top of the EOIS = 33.65 Ma. Thus following the revised definition, the EOT has an estimated duration of 790 kyr. Furthermore, under this definition the ‘Late Eocene event’ is in the base of the EOT.

2. Lithostratigraphy of Site 647

The studied succession belongs to the Lithologic Unit III (Cores 105-647A-15R to 105-647A-55R; 135.4–530.3 mbsf) which is of the middle Eocene to early Oligocene age (Shipboard Scientific Party, 1987) (Fig. S1). The Unit III is grayish-green, moderately to strongly bioturbated nannofossil claystone and nannofossil chalk (Shipboard Scientific Party, 1987). The Subunit IIIA (Cores 105-647A-15R to 105-647A-22r; 135.4–212.3 mbsf) is rich in nannofossil and diatoms. The Subunit IIIB (Cores 105-647A-23R to 105-647A-25R; 212.3–241.1 mbsf) consists of biogenic claystone containing 25%–50% diatoms and sponge spicules. Calcareous nannofossil are present, but not significant. The Subunit IIIC (Cores 105-647A-26R to 105-647A-55R; 241.1–530.3 mbsf) is rich in calcareous nannofossils, on some levels in foraminifers, and yields relatively little biogenic silica. The EOT at Site 647A spans the Subunit IIIC.

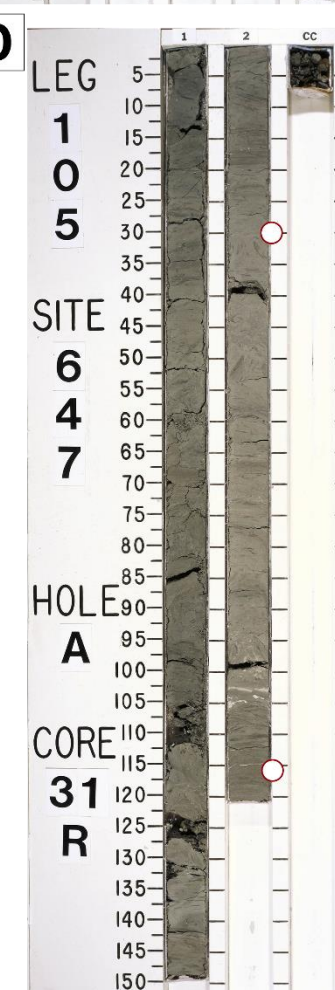
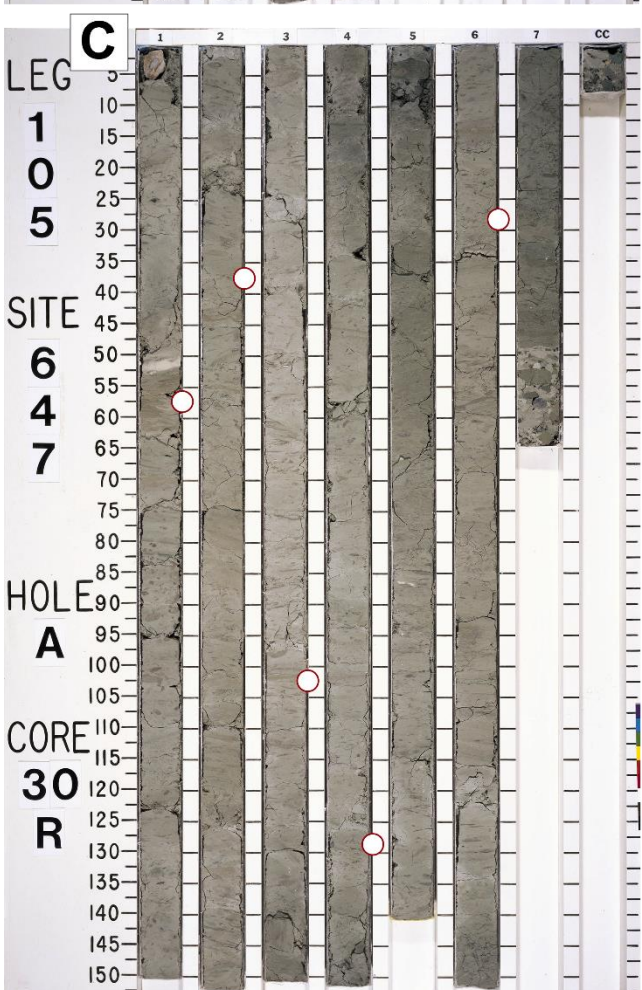
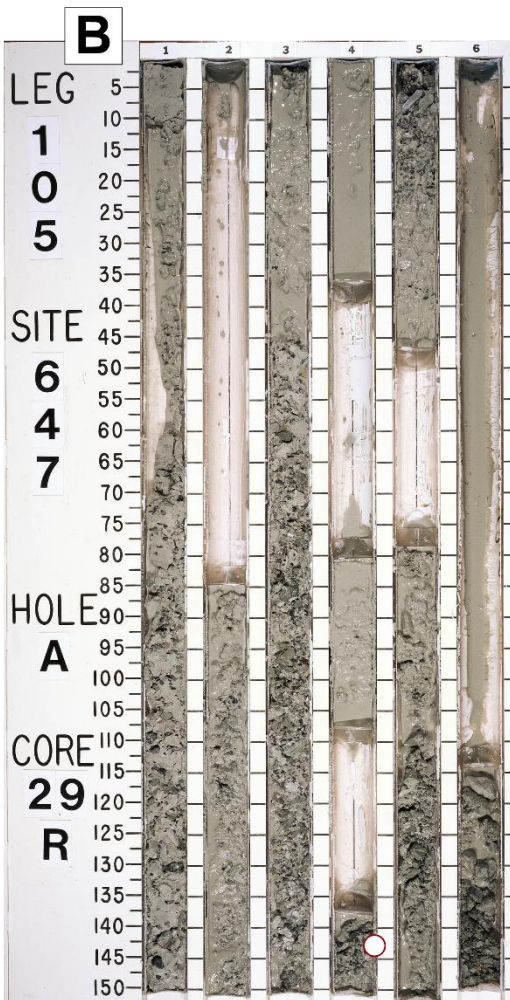
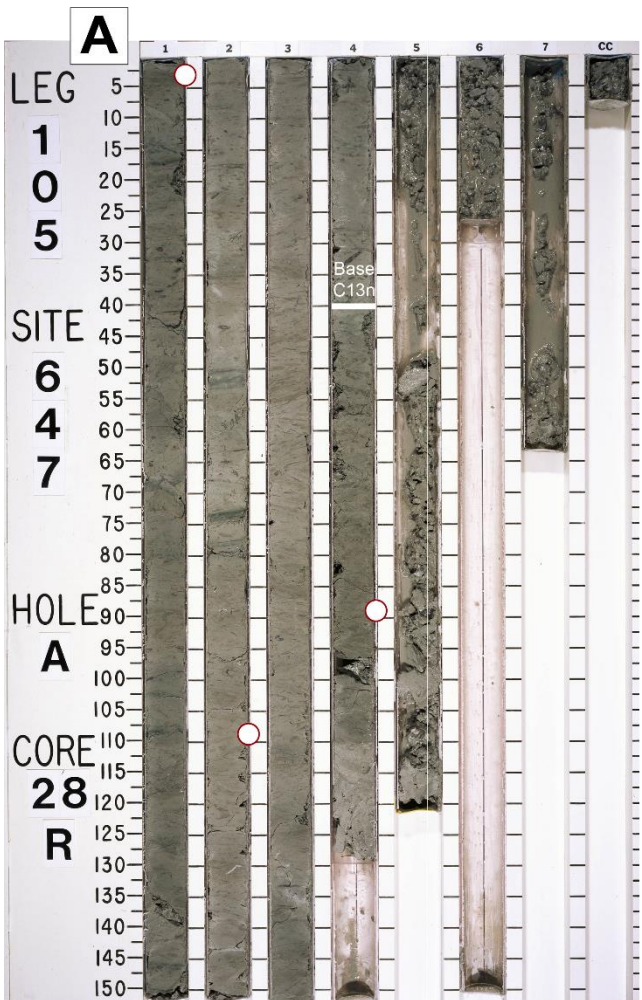


Figure S1:
Photographs of
cores 28 to 31
which span the
Eocene-Oligocene
Transition (EOT)
in the ODP Site
647A. Positioning
of samples for
organic paleo-
thermometry
from these four
cores are marked
with white dots.

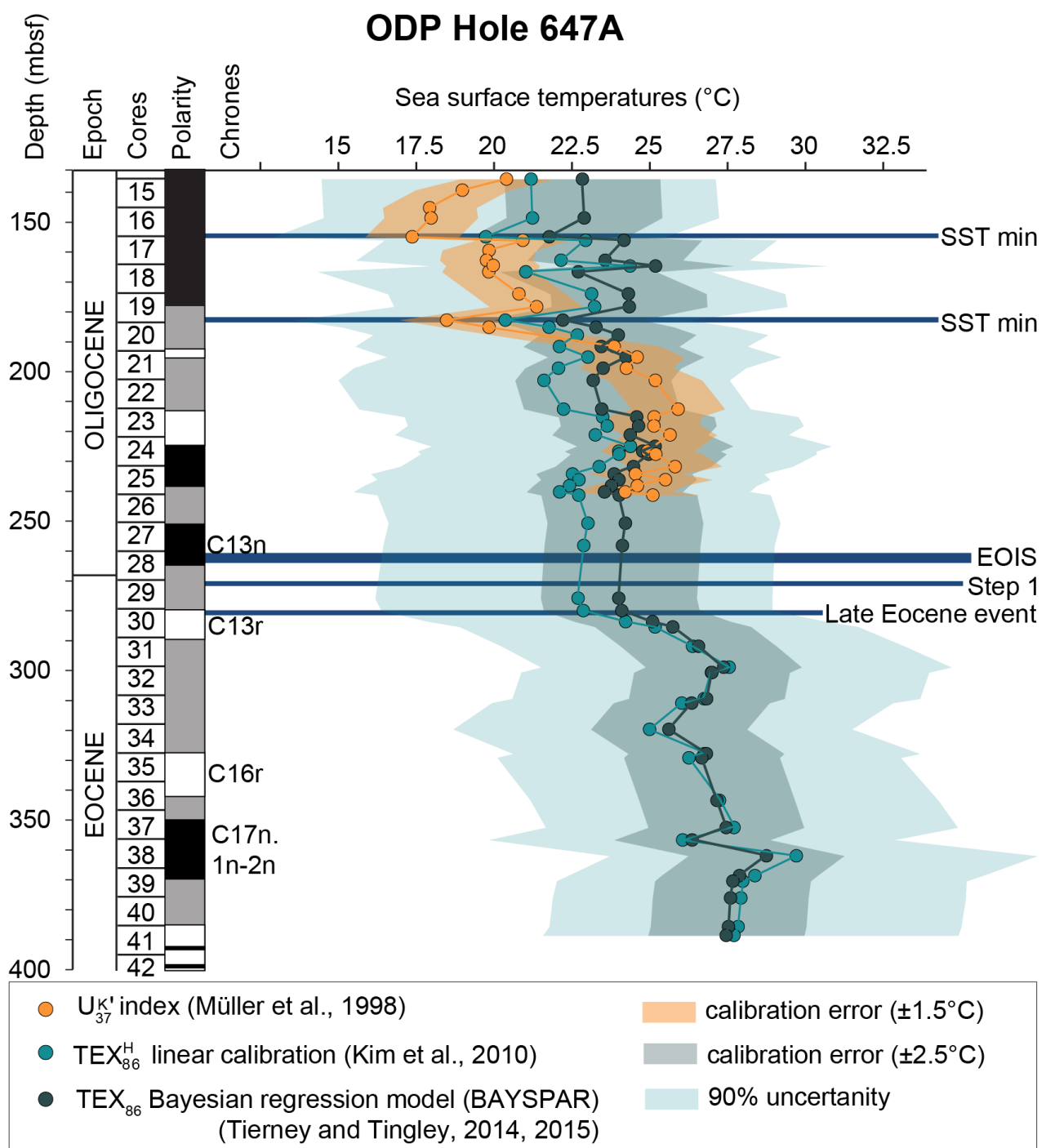


Figure S2: ODP Site 647: chronostratigraphy (Firth et al., 2013) and temperature data (this study) including calibration errors (U_{37}^K and TEX_{86}^H) and 90% uncertainty bar for the BAYSPAR TEX_{86} calibration. Raw data can be found in the Supplements.

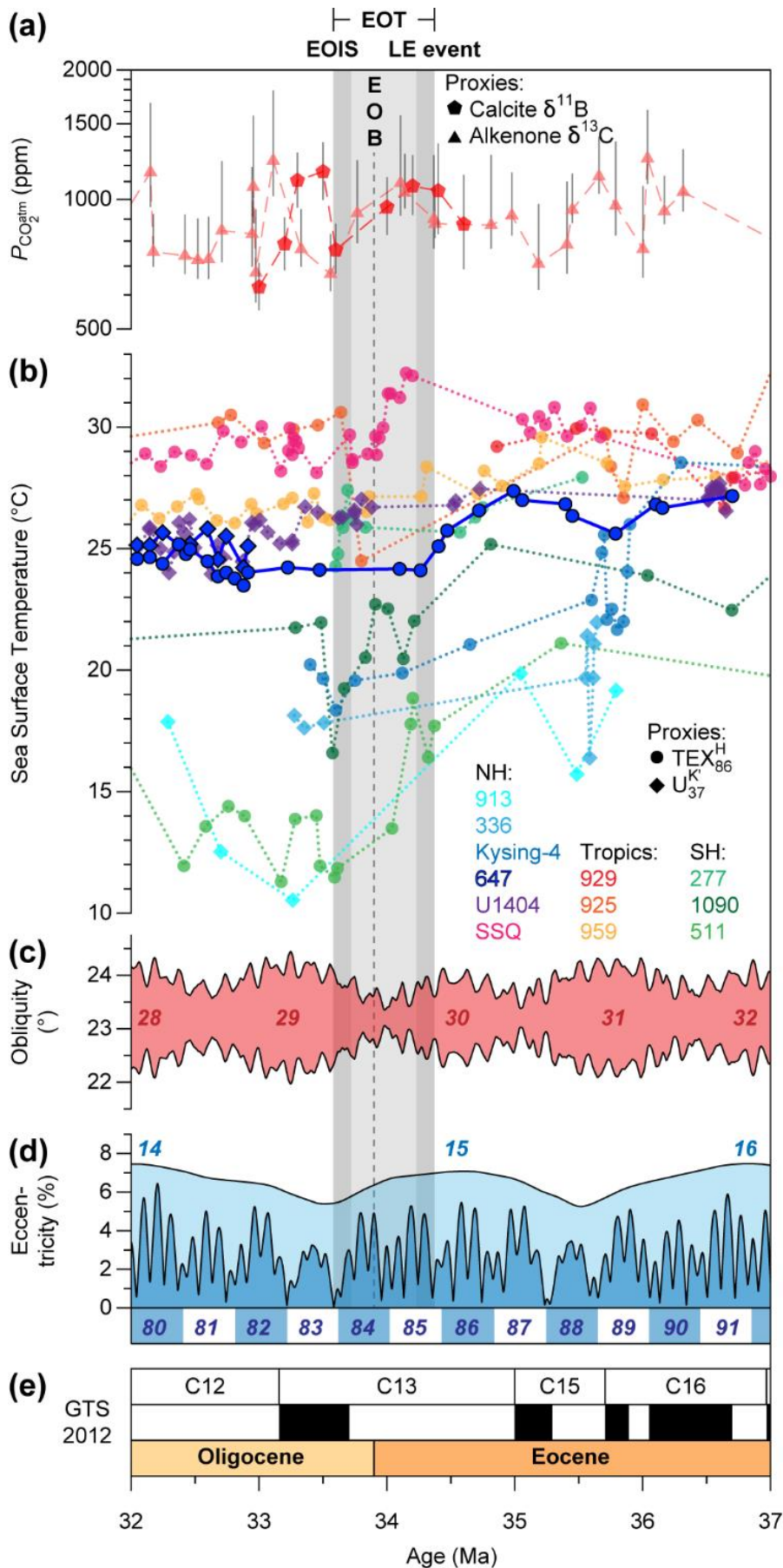


Figure S3: Global SST evolution across the EOT.

(a) Reconstructed $P_{\text{CO}_2^{\text{atm}}}$ based on planktonic foraminiferal $\delta^{11}\text{B}$ (pentagons) (Pearson et al., 2009) and phytoplankton alkenone $\delta^{13}\text{C}$ (triangles) (Pagani et al., 2011; Zhang et al., 2013). The effect of $P_{\text{CO}_2^{\text{atm}}}$ on radiative forcing scales logarithmically.

(b) Newly generated and published (Liu et al., 2009, 2018; Wade et al., 2012; Inglis et al., 2015; Śliwińska et al., 2019; Houben et al., 2019) reconstructed SSTs based on $U_{37}^{k'}$ (diamonds) and $\text{TEX}_{86}^{\text{H}}$ (circles) including Pacific Ocean Site 277 (cf. Fig. 3 in the main document).

(c) ~1.2 Myr obliquity based astrochronozones.

(d) ~2.4 Myr and 405 kyr eccentricity based astrochronozones.

(e) Magneto- and chronostratigraphy based on the GTS2012 (Vandenbergh et al., 2012).

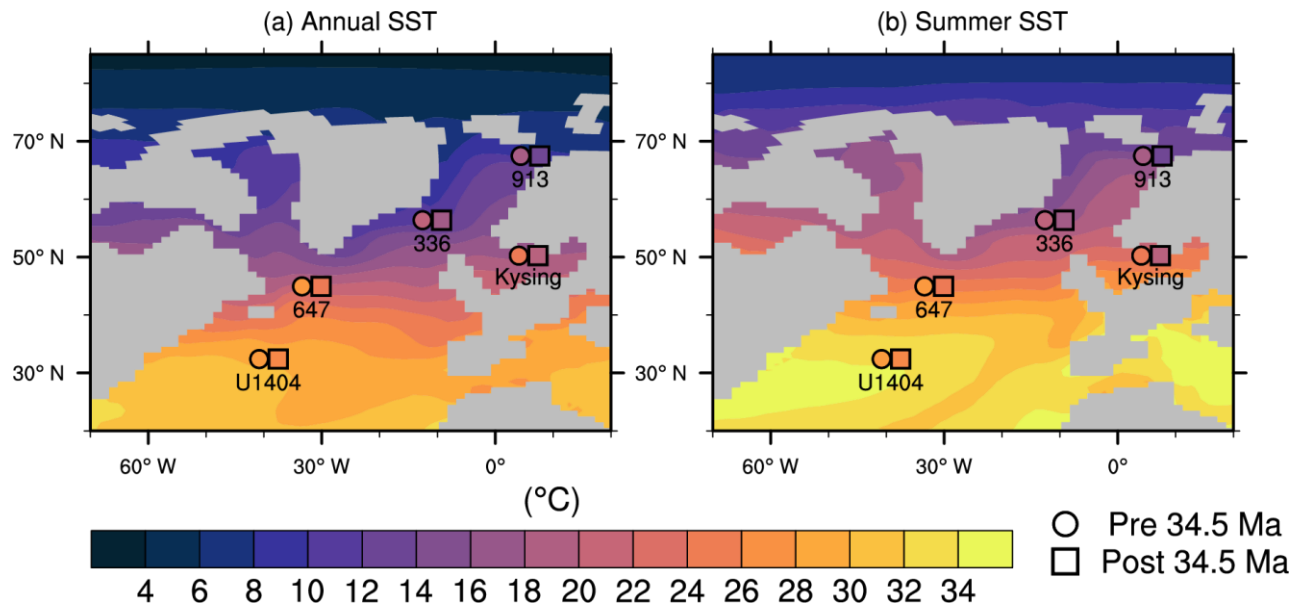


Figure S4: Comparison of the the annual (a) and summer (b) SST in the model control simulation (i.e., Arctic open and 800 ppm CO₂), with site specific SST proxy data: late Eocene (circles; 37 – 34.5 Ma) and early Oligocene (squares; 34.5 – 32 Ma). For details regarding the modelled and proxy SST values see also Figs 4, 6, S5 and the Supplements.

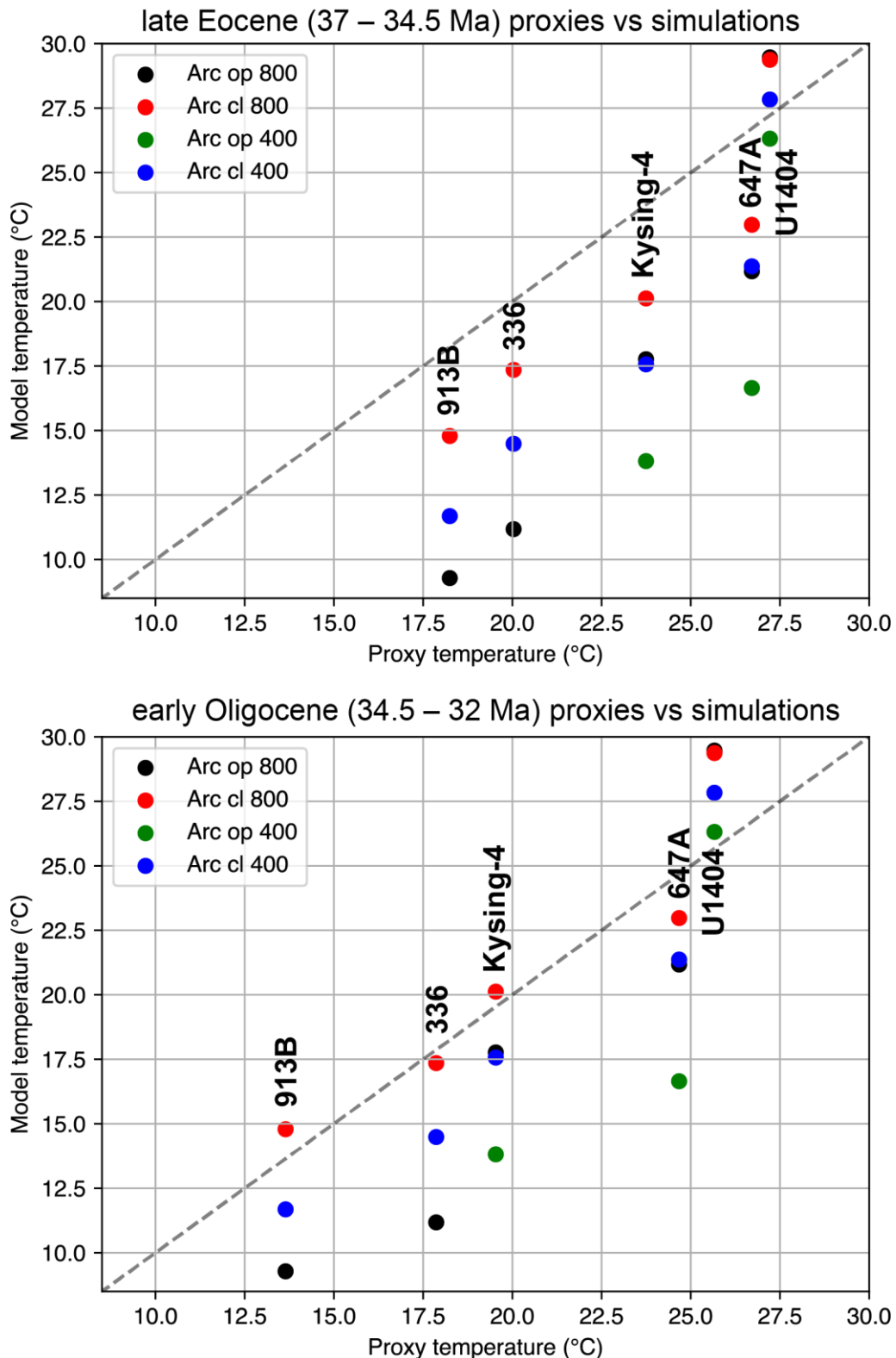


Figure S5: The scatterplot comparison of model annual mean sea surface temperatures with the proxy data. Arc op - Arctic-Atlantic gateway open; Arc cl - Arctic-Atlantic gateway closed; 800 – 800 ppm CO₂ simulation; 400 – 400 ppm CO₂ simulation.

References:

- Firth, J. V., Eldrett, J. S., Harding, I. C., Coxall, H. K., and Wade, B. S.: Integrated biomagnetochronology for the Palaeogene of ODP Hole 647A: implications for correlating palaeoceanographic events from high to low latitudes, Geological Society, London, Special Publications, 373, 29–78, <https://doi.org/10.1144/SP373.9>, 2013.
- Gradstein, F. M., Ogg, J. G., Schmitz, M., and Ogg, G.: The geologic time scale 2012, Elsevier, 2012.
- Houben, A. J. P., Quaijtaal, W., Wade, B. S., Schouten, S., and Brinkhuis, H.: Quantitative organic-walled dinoflagellate cyst stratigraphy across the Eocene-Oligocene Transition in the Gulf of Mexico: A record of climate- and sea level change during the onset of Antarctic glaciation, nos, 52, 131–154, <https://doi.org/10.1127/nos/2018/0455>, 2019.
- Hutchinson, D. K., Coxall, H. K., Lunt, D. J., Steinthorsdottir, M., de Boer, A. M., Baatsen, M., von der Heydt, A., Huber, M., Kennedy-Asser, A. T., Kunzmann, L., Ladant, J.-B., Lear, C. H., Moraweck, K., Pearson, P. N., Piga, E., Pound, M. J., Salzmann, U., Scher, H. D., Sijp, W. P., Śliwińska, K. K., Wilson, P. A., and Zhang, Z.: The Eocene–Oligocene transition: a review of marine and terrestrial proxy data, models and model–data comparisons, Clim. Past, 17, 269–315, <https://doi.org/10.5194/cp-17-269-2021>, 2021.
- Inglis, G. N., Farnsworth, A., Lunt, D., Foster, G. L., Hollis, C. J., Pagani, M., Jardine, P. E., Pearson, P. N., Markwick, P., Galsworthy, A. M. J., Raynham, L., Taylor, Kyle. W. R., and Pancost, R. D.: Descent toward the Icehouse: Eocene sea surface cooling inferred from GDGT distributions, Paleoceanography, 30, 1000–1020, <https://doi.org/10.1002/2014PA002723>, 2015.
- Liu, Z., Pagani, M., Zinniker, D., DeConto, R., Huber, M., Brinkhuis, H., Shah, S. R., Leckie, R. M., and Pearson, A.: Global cooling during the Eocene–Oligocene climate transition, Science, 323, 1187–1190, <https://doi.org/10.1126/science.1166368>, 2009.
- Liu, Z., He, Y., Jiang, Y., Wang, H., Liu, W., Bohaty, S. M., and Wilson, P. A.: Transient temperature asymmetry between hemispheres in the Palaeogene Atlantic Ocean, Nature Geoscience, <https://doi.org/10.1038/s41561-018-0182-9>, 2018.
- Pagani, M., Huber, M., Liu, Z., Bohaty, S. M., Henderiks, J., Sijp, W., Krishnan, S., and DeConto, R. M.: The role of carbon dioxide during the onset of antarctic glaciation, Science, 334, 1261–1264, <https://doi.org/10.1126/science.1203909>, 2011.
- Pearson, P. N., Foster, G. L., and Wade, B. S.: Atmospheric carbon dioxide through the Eocene–Oligocene climate transition, Nature, 461, 1110–1113, 2009.
- Shipboard Scientific Party: Site 647, in: Proc. ODP, Init. Repts., edited by: Srivastava, S. P., Arthur, M., and Clement, B., College Station, TX (Ocean Drilling Program), 675–905, 1987.
- Śliwińska, K. K., Thomsen, E., Schouten, S., Schoon, P. L., and Heilmann-Clausen, C.: Climate- and gateway-driven cooling of Late Eocene to earliest Oligocene sea surface temperatures in the North Sea Basin, Sci Rep, 9, 4458, <https://doi.org/10.1038/s41598-019-41013-7>, 2019.
- Vandenbergh, N., Hilgen, F. J., and Speijer, R. P.: The Paleogene Period, 855–921 pp., <https://doi.org/DOI:10.1016/B978-0-444-59425-9.00028-7>, 2012.
- Wade, B. S., Houben, A. J. P., Quaijtaal, W., Schouten, S., Rosenthal, Y., Miller, K. G., Katz, M. E., Wright, J. D., and Brinkhuis, H.: Multiproxy record of abrupt sea-surface cooling across the Eocene-Oligocene transition in the Gulf of Mexico, Geology, 40, 159–162, <https://doi.org/10.1130/G32577.1>, 2012.
- Zhang, Y. G., Pagani, M., Liu, Z., Bohaty, S. M., and DeConto, R.: A 40-million-year history of atmospheric CO₂, Philosophical Transactions of the Royal Society A: Mathematical, Physical and Engineering Sciences, 371, 2013.